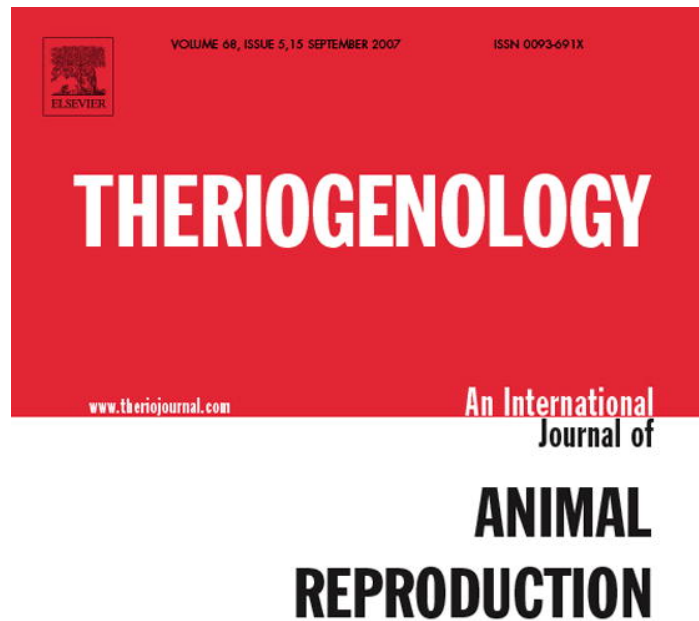


Provided for non-commercial research and education use.
Not for reproduction, distribution or commercial use.



The Official Journal of the
Society for
Theriogenology
Veterinarians Dedicated to Animal Reproduction

This article was published in an Elsevier journal. The attached copy is furnished to the author for non-commercial research and education use, including for instruction at the author's institution, sharing with colleagues and providing to institution administration.

Other uses, including reproduction and distribution, or selling or licensing copies, or posting to personal, institutional or third party websites are prohibited.

In most cases authors are permitted to post their version of the article (e.g. in Word or Tex form) to their personal website or institutional repository. Authors requiring further information regarding Elsevier's archiving and manuscript policies are encouraged to visit:

<http://www.elsevier.com/copyright>



ELSEVIER

Available online at www.sciencedirect.com

Theriogenology 68 (2007) 804–812

Theriogenology

www.theriojournal.com

Rapidly cooled horse spermatozoa: Loss of viability is due to osmotic imbalance during thawing, not intracellular ice formation

G.J. Morris^{a,*}, K. Faszer^a, J.E. Green^b, D. Draper^b, B.W.W. Grout^{b,1}, F. Fonseca^c

^a *Asymptote Ltd., St John's Innovation Centre, Cowley Road, Cambridge CB4 0WS, UK*

^b *Postgraduate School, Writtle College, Chelmsford, CM1 3RR, UK*

^c *UMR Genie et Microbiologie des Procédés Alimentaires, Institute National de la Recherche Agronomique, Institute National Agronomique, Paris-Grignon, F-78850 Thierval-Grignon, France*

Received 7 January 2007; received in revised form 4 May 2007

Abstract

The cellular damage that spermatozoa encounter at rapid rates of cooling has often been attributed to the formation of intracellular ice. However, no direct evidence of intracellular ice has been presented. An alternative mechanism has been proposed by Morris (2006) that cell damage is a result of an osmotic imbalance encountered during thawing. This paper examines whether intracellular ice forms during rapid cooling or if an alternative mechanism is present. Horse spermatozoa were cooled at a range of cooling rates from 0.3 to 3000 °C/min in the presence of a cryoprotectant. The ultrastructure of the samples was examined by Cryo Scanning Electron Microscopy (CryoSEM) and freeze substitution, to determine whether intracellular ice formed and to examine alternative mechanisms of cell injury during rapid cooling. No intracellular ice formation was detected at any cooling rate. Differential scanning Calorimetry (DSC) was employed to examine the amount of ice formed at different rate of cooling. It is concluded that cell damage to horse spermatozoa, at cooling rates of up to 3000 °C/min, is not caused by intracellular ice formation. Spermatozoa that have been cooled at high rates are subjected to an osmotic shock when they are thawed.

© 2007 Elsevier Inc. All rights reserved.

Keywords: Horse spermatozoa; Cryopreservation; Intracellular ice; Osmotic imbalance

1. Introduction

Methods for the cryopreservation of spermatozoa need to be improved for many medical, veterinary and conservation applications. In order to develop protocols to maximize recovery on thawing it is essential to understand the events which lead to cellular injury during freezing and thawing, none less so than for equine spermatozoa [2,8,37].

The physical stresses important in determining the cellular response during cryopreservation are well documented. Following ice formation in the extracellular solution, all solutes and suspended materials, including cells, become localised into freeze concentrated compartments [25]. During the subsequent reduction in temperature, cells are exposed to increasingly concentrated solutions. This process continues until the freeze concentrated solution crystallises as a eutectic, or becomes a glass. The hypertonic conditions that cells encounter lead to an osmotic loss of water, the extent of which is dependent on the rate of cooling.

With many cell types, including mammalian oocytes and embryos, the osmotic behaviour of the cell during freezing may be predicted from numerical models. In

* Corresponding author. Tel.: +44 1223 421161; fax: +44 1223 421166.

E-mail address: jmorris@asymptote.co.uk (G.J. Morris).

¹ Present address: Faculty of Life Sciences, University of Copenhagen, Højbakkegaard Alle 9, 2630 Taastrup, Denmark.

particular, the probability of intracellular ice formation for different linear rates of cooling may be estimated. The models correlate with light cryomicroscopy studies, which allow the visualization of intracellular ice in oocytes and embryos at different rates of cooling [25]. However, experimental observations of mammalian spermatozoa cryopreserved in glycerol have not been in agreement with the results predicted from modelling [9,11,18,26,32]. The models assume that damage to spermatozoa at rapid rates of cooling is due to the formation of intracellular ice. Recently [28] it has been demonstrated that rapid cooling of cryoprotected human spermatozoa leads to loss of viability in the absence of intracellular ice, cellular damage observed after rapid cooling rates was caused by an osmotic imbalance encountered during thawing. A similar explanation for the damage observed with rapidly cooled bacteria has been proposed [16].

In this investigation we have examined whether the response of horse spermatozoa suspended in a glycerol cryoprotectant [24] cooled at different rates can be explained by this alternative model of injury. The viability following different cooling rates was compared with the ultrastructure in the frozen state as determined by freeze fracture and freeze substitution electron microscopy. The amount of ice formed at different rates was measured by differential scanning calorimetry allowing the extent of any osmotic balance on thawing to be estimated.

2. Materials and methods

2.1. Semen samples and experimental design

Semen was collected from a 4-year-old Fell Pony stallion and processed in the conventional way to provide a gel-free sperm pellet, centrifuged from Kenny extender (Minitub, Abfull-und Labortechnik GmbH & Co., Tiefenbach, Germany) at 2:1 extender:sperm. The recovered pellet was re-extended with a Gent, glycerol-based freezing medium (Minitub, Abfull-und Labortechnik GmbH & Co, Germany) to a concentration of 1.6×10^8 sperm/ml and loaded into straws (0.25 ml). The loaded straws were placed horizontally at 4 °C for 3 h in a standard laboratory refrigerator.

Following preliminary experiments to establish the range of cooling rates of interest all the viability, freeze substitution and freeze fracture data presented in this paper were obtained with a single ejaculate. Any sample-to-sample variation was thus avoided.

2.2. Semen analysis and sperm function testing

Sperm motility and viability were assessed using a SpermVision™ Computer Assisted Sperm Analysis (MTG-Medical Technology Vertriebs-GmbH, Altdorf, Germany) based on a Zeiss Axiosko 40FL fluorescence microscope. Percentage motility was recorded as all moving sperm in the semen sample. Percentage viability was assessed, using the CASA system, following dual staining with SYBR14 and propidium iodide using a proprietary sperm viability kit (L-7011 Invitrogen Ltd., Paisley, UK). At least 10 straws were examined for each freezing and thawing treatment.

2.3. Freezing

All samples underwent the same cooling process until ice nucleation: straws were cooled from 4 to –7 °C at a rate of 2 °C/min in an Asymptote EF600 freezer (Asymptote Ltd., Cambridge, UK) and then maintained at –7 °C for 10 min during which time a small cryosurgical device (Asymptote Ltd., Cambridge, UK), was used to nucleate individual straws *in situ* on the cooling plate of the Stirling Cycle freezer [15]. Samples were then cooled at various rates. Samples cooled at rates of up to 30 °C/min were cooled on the sample plate of the EF600 freezer until they reached a temperature of –100 °C, at which point they were transferred to liquid nitrogen for storage. For rates of cooling between 30 and 50 °C/min straws were cooled in a Planer controlled rate freezer. Samples nucleated on the sample plate of the EF600 were cooled at rates faster than 50 °C/min using methods described previously [30]. Temperatures were measured and logged in the samples using a type T 28 SWG thermocouples connected to a 1200 series Grant data logger (Grant Instruments, Cambridge, UK) or a Pico TC-08 data logger (Pico Technology Ltd., St Neots, Cambs, UK).

2.4. Thawing and post-thaw semen assessment

Generally straws were thawed in a water bath at 37 °C for 30 s, in one experiment the effect of different warming rates on the viability of straws that had been frozen at 10 °C/min this was achieved by transferring straws to the sample plate of a EF600 freezer maintained at –100 °C and warming at controlled rates.

2.5. Freeze fracture electron microscopy

Straws were frozen as above, freeze fractured and loaded onto a CryoSEM stage (Oxford Instruments

XL30-FEG). The stage was warmed from $-145\text{ }^{\circ}\text{C}$ to $-90\text{ }^{\circ}\text{C}$ over 6 min and the sample etched at $-90\text{ }^{\circ}\text{C}$ for 6 min before cooling to $-145\text{ }^{\circ}\text{C}$. The sample was then transferred to a preparation stage, coated with 10–15 nm gold and loaded back onto the CryoSEM stage for image recording [29]. The ice fraction of the sample (external to the freeze concentrated material) was calculated from the micrographs [31].

2.6. Freeze substitution

Straws were freeze substituted in a Reichert automated freeze substitution chamber, samples were maintained at $-90\text{ }^{\circ}\text{C}$ for 24 h, warmed to $-70\text{ }^{\circ}\text{C}$ at $3\text{ }^{\circ}\text{C/h}$ and then maintained at $-70\text{ }^{\circ}\text{C}$ for 24 h. Samples were then warmed to room temperature at $3\text{ }^{\circ}\text{C/h}$, rinsed in methyl alcohol and embedded in Spurr's epoxy resin [29]. Sections $0.5\text{ }\mu\text{m}$ thick were prepared with a Reichert Ultracut S microtome and stained with methylene blue.

2.7. Differential scanning calorimetry (DSC)

DSC measurements of the ice fraction at different rates of cooling were carried out using a power compensation DSC (Pyris 1, Perkin-Elmer LLC, Norwalk, CT, USA) equipped with a liquid nitrogen-cooling accessory [31]. Linear cooling and heating rates varying from 1 to $300\text{ }^{\circ}\text{C/min}$ were used throughout these DSC studies. Temperature calibration was done using cyclohexane (crystal–crystal transition at $-87.1\text{ }^{\circ}\text{C}$) and mercury (melting point $-38.6\text{ }^{\circ}\text{C}$) for the heating rates studied. Mercury was also used for energy calibration (11.8 J/g crystallization/melting) and for verifying during cooling the fitting of the calibration made with heating data (less than $2\text{ }^{\circ}\text{C}$ difference between rates of cooling of 1 and $300\text{ }^{\circ}\text{C/min}$ and no difference in energy). This equipment allows measuring the program temperature and the sample temperature, thus making possible the estimation of the range of linearity of the sample cooling rates. For instance, when cooling at $100\text{ }^{\circ}\text{C/min}$ this controlled cooling rate is followed by the sample from $25\text{ }^{\circ}\text{C}$ down to $-140\text{ }^{\circ}\text{C}$, while at $250\text{ }^{\circ}\text{C/min}$, the range is reduced to $25\text{ }^{\circ}\text{C}$ to $-75\text{ }^{\circ}\text{C}$. Samples of about 5 mg were cooled to $-175\text{ }^{\circ}\text{C}$ and scanned to $25\text{ }^{\circ}\text{C}$. SnowMax, a freeze dried preparation of *Pseudomonas syringae* (York Snow, Victor, NY, USA) was added to initiate ice formation during cooling [38].

In order to understand the complex transitions observed at rapid rates of cooling some samples were cooled in the DSC in a conventional manner, warmed to $-7\text{ }^{\circ}\text{C}$ and then cooled at the same rate.

3. Results

3.1. Effect of cooling rate on recovery of sperm

The motility of horse spermatozoa had a broad optimum between 4 and $50\text{ }^{\circ}\text{C/min}$, at both faster and slower rates of cooling the viability decreased. In particular, at rates of cooling faster than $150\text{ }^{\circ}\text{C/min}$ the viability decreased rapidly with increasing cooling rate. The viability of the same sample as determined by SYBR14 and propidium iodide was c.a. 50% at rates of cooling between 4 and $50\text{ }^{\circ}\text{C/min}$ (Fig. 1). At rates of cooling greater than $50\text{ }^{\circ}\text{C/min}$ the viability and motility data were very similar. However, at rates of cooling slower than $50\text{ }^{\circ}\text{C/min}$, the values for motility were lower than viability.

3.2. Effect of warming rate on viability of sperm

The effect of rate of warming on the recovery of horse spermatozoa that had been cooled at a rate of $10\text{ }^{\circ}\text{C/min}$ was examined (Fig. 2). The viability was maximum at the fastest rates of warming examined (50%) and decreased to below 10% as the warming rate decreased. The motility of the same sample showed a greater sensitivity to the rate of warming than the viability data.

3.3. Structure of the frozen sample at different cooling rates

Cross fracture of straws frozen in glycerol cryoprotectant, followed by deep etching to remove crystalline

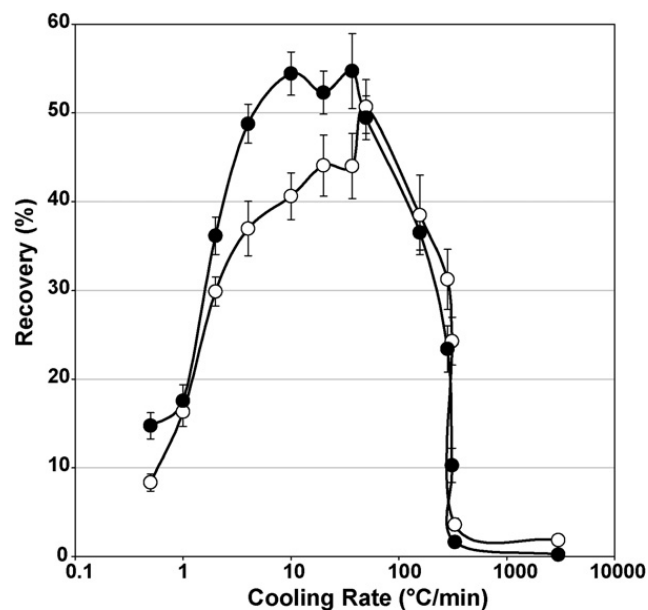


Fig. 1. Motility (●) and viability (○) of horse spermatozoa following different rates of cooling. All samples thawed rapidly.

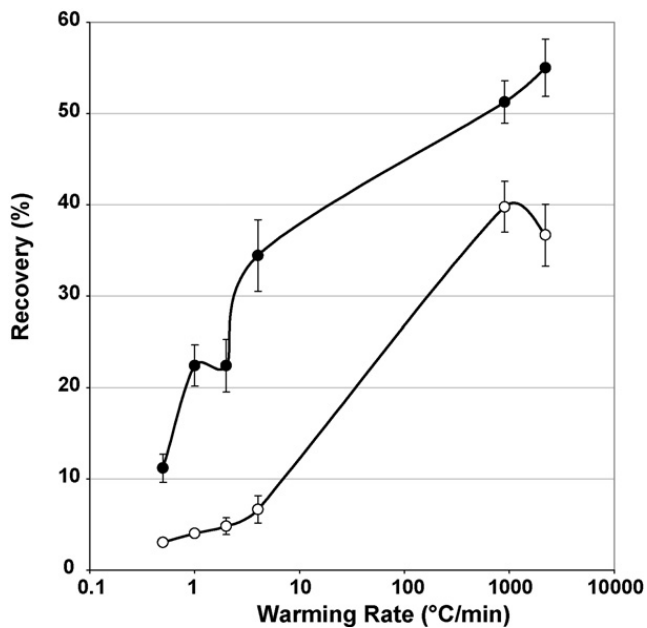


Fig. 2. Motility (●) and viability (○) of horse spermatozoa following different rates of warming. All samples initially cooled at 10 °C/min.

ice, revealed the structure of the freeze concentrated cryoprotectant. After ice nucleation at -7°C and a subsequent cooling rate of $10^{\circ}\text{C}/\text{min}$, a cross-section of a straw revealed extensive ice formation (Fig. 3a). The domains of freeze concentrated material were homogeneous in structure (Fig. 3b). Generally few spermatozoa were apparent, although some were associated with the interface between the freeze concentrated material and ice crystals. Some sperm tails were observed to extend away from the freeze concentrated material suggesting that these structures were associated with or entrapped in ice (Fig. 3b). Samples that were nucleated at -7°C and then cooled at a rate of $3000^{\circ}\text{C}/\text{min}$ had a freeze concentrated material which occupied a much larger cross-sectional area (Fig. 3e) and contained numerous ice crystals, evident as etched pits and dendrites (Fig. 3f). In these samples spermatozoa were not evident. Cross fracture of samples frozen at $330^{\circ}\text{C}/\text{min}$ revealed an intermediate structure, with more ice within the sample than following rapid cooling (Fig. 3c) some portions of the freeze concentrated material contained ice whilst adjacent sections were ice free (Fig. 3d). The ice crystals were approximately $2\ \mu\text{m}$ in diameter and regular in appearance, although they appear contiguous they are not obviously dendritic. At this cooling rate the interface between the freeze concentrated material and ice often was smooth with a distinct “wall” structure.

After cooling rates of $10^{\circ}\text{C}/\text{min}$, the ice fraction (external to the freeze concentrated material) was measured to be 67%. After rapid cooling (330 and $3000^{\circ}\text{C}/\text{min}$), the ice fraction external to the freeze concentrated material was 63 and 49% respectively. At the rapid rates of cooling crystalline ice also formed within the freeze concentrated material but it was not possible to quantify this.

3.4. Electron microscopy of cells following different cooling rates

Electron microscopy of freeze-substituted samples frozen at a cooling rate of $10^{\circ}\text{C}/\text{min}$ showed some cell dehydration and distortion, and the cytoplasm and organelles appeared dense (Fig. 4a and b). At a cooling rates of 330 and $3000^{\circ}\text{C}/\text{min}$ there was no evidence of ice within any compartment of the cell, within the resolution limits of the techniques (Fig. 4c–f).

3.5. Differential scanning calorimetry

At rates of cooling between 10 and $250^{\circ}\text{C}/\text{min}$ the ice fraction formed during cooling was somewhat variable but always above 0.7 (Fig. 5). At rates of cooling greater than $250^{\circ}\text{C}/\text{min}$ the ice fraction formed during freezing decreased. On warming the equilibrium amount of ice melted in all samples, even following rapid cooling.

When cooling at low cooling rates (5 – $100^{\circ}\text{C}/\text{min}$) only one large freezing event is observed. At faster rates of cooling other transitions are observed by DSC

1. Between cooling rates of 200 – $260^{\circ}\text{C}/\text{min}$ there is the initial exothermic event followed by two smaller events. The first of these events occurs around -41°C and is clearly an exothermic event. The second occurs at -80°C at a cooling rate of $200^{\circ}\text{C}/\text{min}$ and -55°C at a cooling rate of $260^{\circ}\text{C}/\text{min}$ and appears to be either an endothermic event or the overlapping of an endothermic and an exothermic one (Fig. 6). The thermal event at -41°C disappeared in samples that had been annealed by warming back to -7°C and then again cooled rapidly.
2. Between cooling rates of 270 – $280^{\circ}\text{C}/\text{min}$ there is only one smaller event occurring around from -42°C to -60°C (the higher the cooling rate, the lower the event temperature).
3. Between cooling rates of 280 – $300^{\circ}\text{C}/\text{min}$ there is only one smaller exothermic event occurring around -60°C .

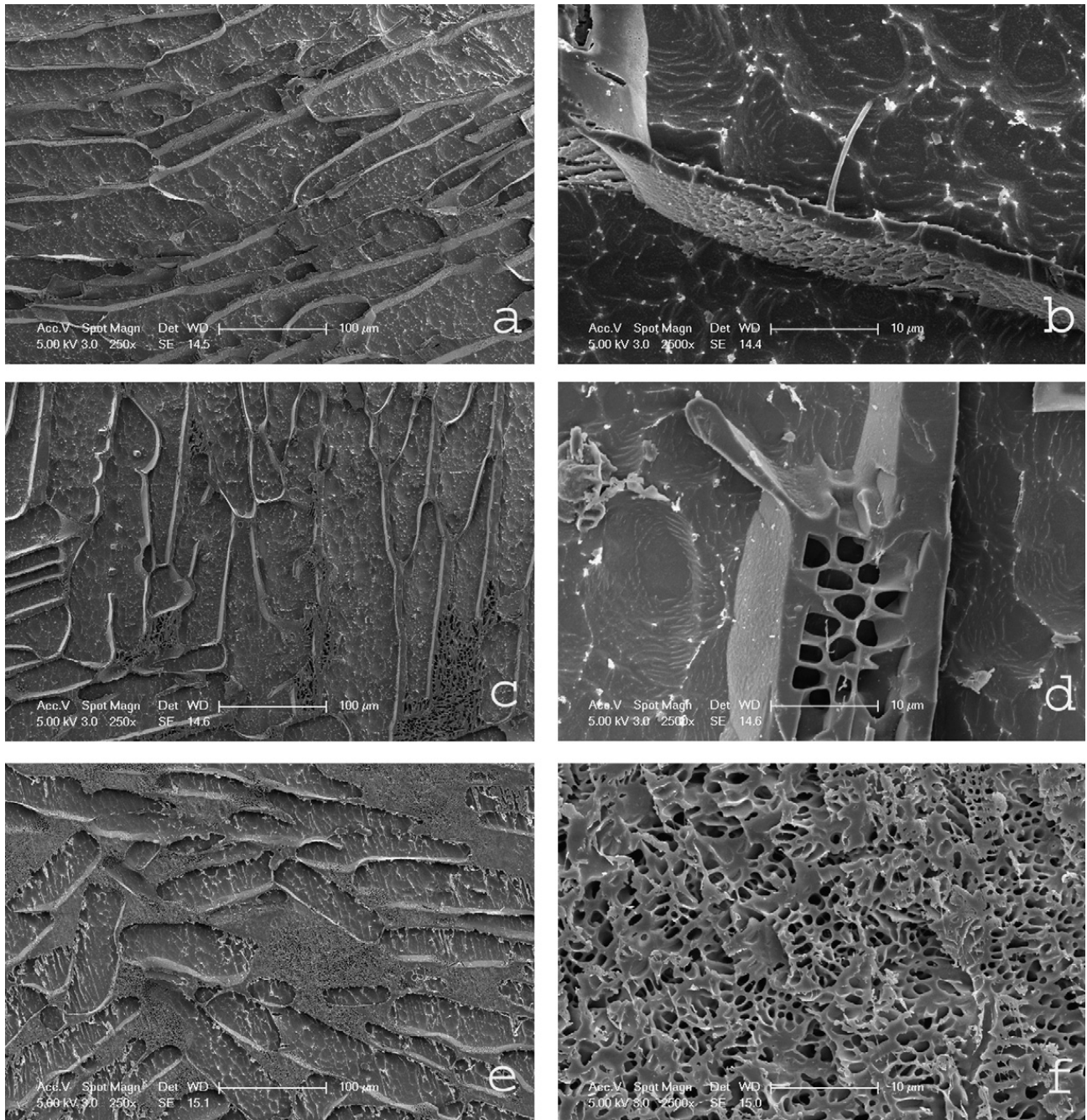


Fig. 3. CryoSEM of cryopreserved horse spermatozoa cooled with glycerol cryoprotectant at 10 °C/min (a and b), 330 °C/min (c and d), and 3000 °C/min (e and f).

4. Discussion

There have been surprisingly few publications on the effect of cooling rate on the recovery rate of horse spermatozoa [13,14,27,35] and the viability data presented here (Fig. 1) is similar to that previously published [12]. The observed differences in the viability and motility measurements suggest that different mechanisms of cellular injury may be occurring at “slow” and “rapid” rates of cooling. The effect of

warming rate on frozen horse spermatozoa (Fig. 2) is similar to that reported for human sperm [19]. Recovery of motility appears to be more sensitive to damage at slow rates of warming than does viability. A large variation has been reported between stallions in the response of their spermatozoa to freezing and thawing [8,35]. In this study we have examined the primary cause of freezing injury at rapid rates of cooling for one stallion, we intend to examine the behavior of other stallions at rapid rates of cooling.

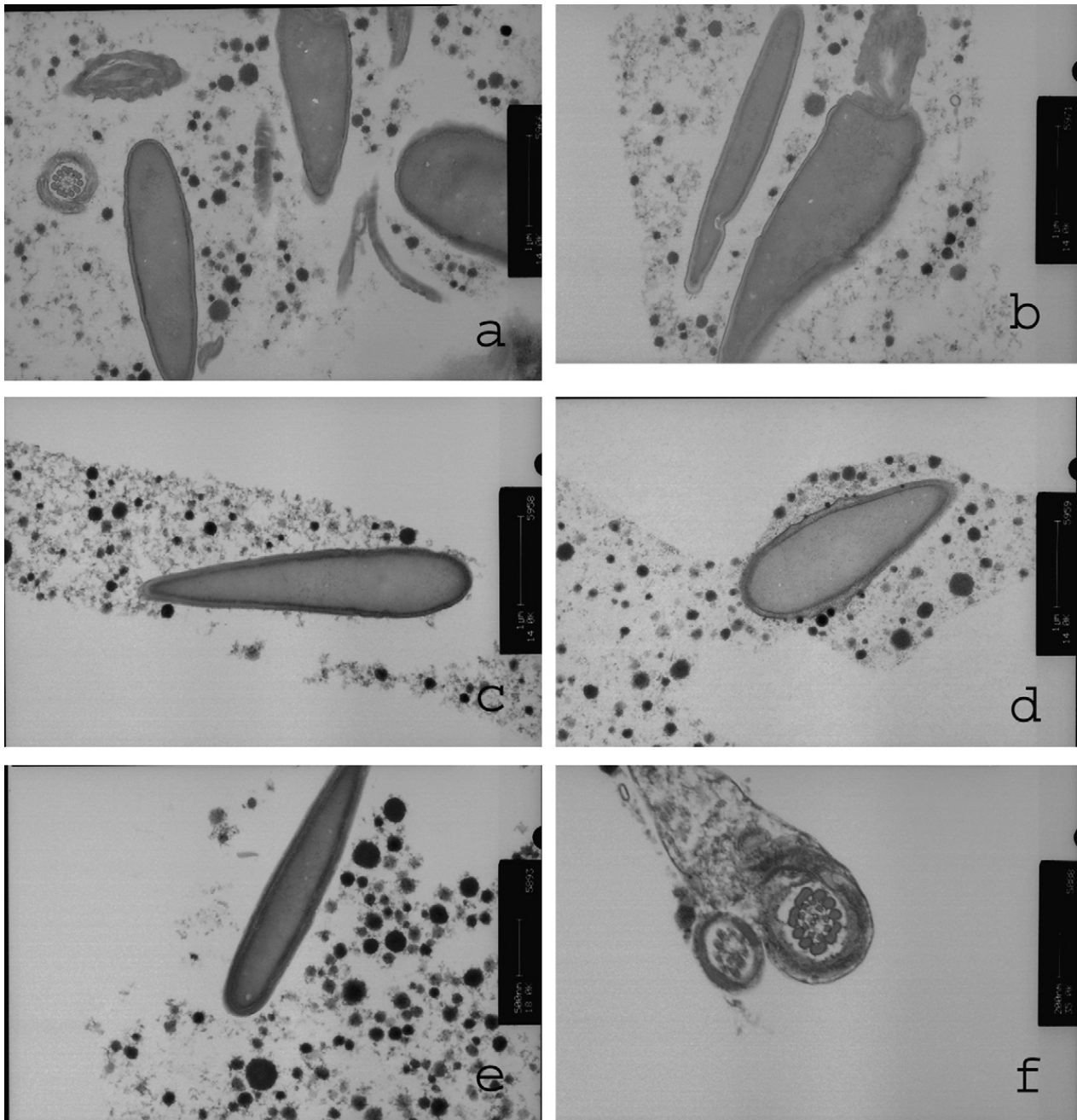


Fig. 4. Freeze substitution of cryopreserved horse spermatozoa cooled 10 °C/min (a and b), 330 °C/min (c and d), and 3000 °C/min (e and f).

In this study there is no evidence that the reduction in viability to <2% following rapid rates of cooling (330 and 3000 °C/min) is caused by the formation of intracellular ice. At these rapid rates of cooling there is no evidence from either freeze fracture or freeze substitution of intracellular ice formation. Studies on freeze substitution and freeze fracture of cryopreserved pig spermatozoa [7,34] human spermatozoa [28,29] and freeze substitution of slowly frozen testicular spermatozoa within the mouse epididymis [36] have been reported. In these reports, though some intracellular ice formation within sperm tails and midpieces of pig and

mouse spermatozoa was evident, there was no evidence for gross ice formation within the sperm heads.

If intracellular ice is not the cause of cell damage at rapid rates of cooling, other physical events must be responsible. The most important factors in the reduction of viability are changes in the physical properties of the extracellular environment.

It has been demonstrated that freezing an aqueous solution of glycerol causes the viscosity of the freeze concentrated material to increase rapidly [31]. Following ice nucleation, the growth of ice crystals in an aqueous solution occurs by the diffusion of water

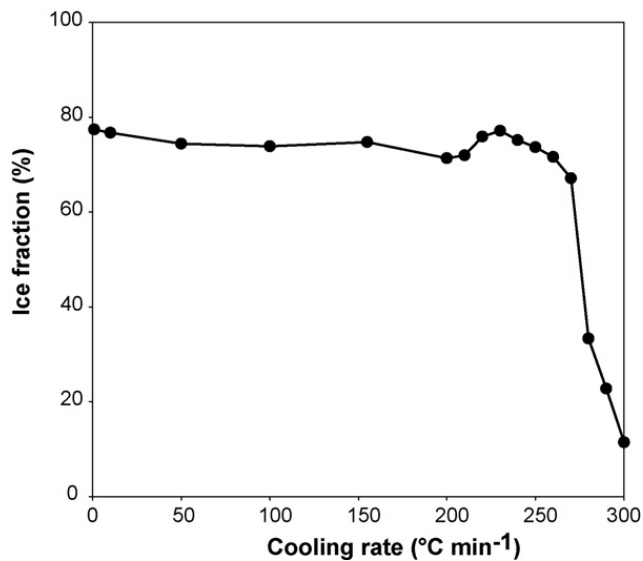


Fig. 5. Amount of ice formed (g ice/g total water) in a horse sperm extender cooled at different rates.

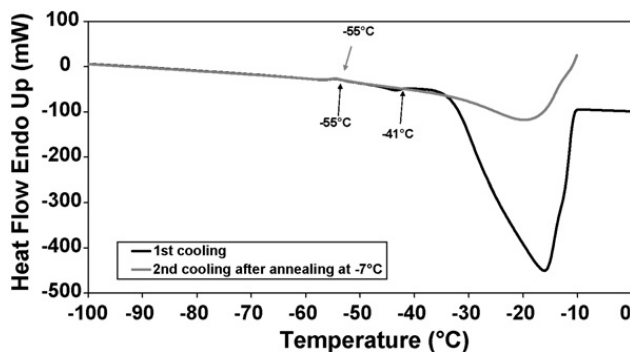


Fig. 6. DSC thermogram following cooling at rapid rates, for a horse sperm extender.

molecules from the solution adjacent to the ice crystal to the ice crystal lattice. As the viscosity of the solution increases during freezing this diffusion process may become limited and the amount of ice formed then becomes dependent on the rate of cooling—so called diffusion-limited crystallization. The relationship between the rate of cooling and the amount of ice formed has been quantified for some defined cryoprotectant systems [4,5,31] and for the complex extender used in this work (Fig. 5). The data obtained with the glycerol based extender used in this study was similar to that previously reported [31] for 10% glycerol in 0.15 M NaCl.

The ultrastructure of the frozen sperm sample differed according to the rate the sample was cooled following nucleation and image analysis provided confirmation of the DSC data. Samples that were cooled at 10 °C/min had a homogeneous freeze concentrated material with an ice fraction external of 67%. However, at faster rates of cooling (330 and 3000 °C/min), the ice fraction was 67%

and 49% respectively. At high rates of cooling, the freeze concentrated material becomes “supercooled”. At some temperature during cooling, ice nucleation occurs within this material, trapping the water as ice within the freeze concentrated solution [31].

It may also be noted that in samples in which controlled ice nucleation was induced and then cooled rapidly, it would be expected that concentration gradients would be established within the freeze concentrated material during cooling. The highest glycerol concentration would be at interface between the freeze concentrated material and the ice and it would be lowest in the middle of the domain, leading to constitutional supercooling [10]. The ultrastructure of samples cooled at a rate of 330 °C/min⁻¹ (Fig. 3d) is consistent with constitutional supercooling. It is therefore likely that cells at different positions within the freeze concentrated material will be encounter different concentration gradients during freezing and thawing. It would be expected that the viability of cells on thawing is determined by the local environment, not by the averaged value for the sample.

It is not apparent from this study when ice nucleation occurs within the “supercooled” freeze concentrated matrix of rapidly cooled samples. At low temperatures, the freeze concentrated matrix of rapidly cooled samples will be surrounded by ice and may have a concentration at the ice:freeze concentrated matrix interface which does not allow “seeding” of the freeze concentrated matrix from the ice crystals. The freeze concentrated matrix may then undercool significantly and the studies on the nucleation of ice in concentrated solutions of glycerol [20,21,39] and ethylene glycol [3,6] become relevant.

It has been reported [39] that in a 50 wt% solution of glycerol, ice nucleation without growth continues at -110 °C and two forms of ice appear simultaneously (approximately 30% of hexagonal ice and 70% cubic ice nuclei).

DSC curves following rapid freezing (Fig. 6) indicate complex transitions within the freeze concentrated matrix. Similar transitions have been reported during the freezing of concentrated solutions of ethylene glycol [3]. However, how these transitions relate to any nucleation events within the freeze concentrated matrix is not clear and requires further study.

Whatever the temperature of nucleation of the ice in the freeze concentrated material following rapid rates of cooling the cells will reach low temperatures suspended in a non-equilibrium concentration. During warming of rapidly cooled bulk glycerol solutions, containing metastable solid states, a number of recrystallisation

patterns have been described [1,17,23]. Following the rapid cooling of human spermatozoa [31] CryoSEM and DSC demonstrates that during warming of rapidly cooled samples migratory recrystallisation of the ice occurs.

The sequence of events described above allows a model of injury to be described which is determined solely by the solidification processes within the suspending medium. At slow rates of cooling and with ice nucleation at temperatures close to the melting point, the cells are exposed at all temperatures to the concentration of glycerol predicted from the equilibrium phase diagram. At T_g the glycerol solution will vitrify. On warming, the cell environment is diluted from the maximally concentrated solution to the original concentration. At very slow rates of cooling the cells are exposed to hypertonic solutions for long periods and cell death will occur. As the rate of cooling increases the exposure time during cooling decreases and the viability increases. However, as the cooling rate is further increased the amount of ice formed during freezing deviates from the equilibrium value, and at any temperature during rapid cooling the cells are exposed to a concentration of glycerol lower than the value predicted from the equilibrium phase diagram. At some unknown temperature (above or below T_g) ice nucleates within the freeze concentrated material and the concentration of the glycerol and other solutes then attains a more concentrated value and vitrifies. On warming above T_g , the cells, which have been suspended in a non-equilibrium concentration of glycerol during cooling, are exposed to the equilibrium concentration of glycerol. Cells may be able to tolerate a small osmotic shock, but as the magnitude increases such osmotic shock will become damaging [33]. A comparison of the viability of horse sperm on thawing (Fig. 1) compared with the amount of ice formed during cooling (Fig. 5) clearly shows that at rates of cooling at which the composition of the extracellular matrix deviates from equilibrium values correlates with loss of viability.

The response of spermatozoa of several mammalian species cryopreserved in the presence of glycerol have very common pattern when plotted against cooling rate [22]. Even though sperm cells of different species have different morphology, surface area to volume ratios, coefficient of water permeability and activation energy for water permeability etc the viability declines rapidly once a critical cooling rate of approximately 100 °C/min has been exceeded [22]. However, there is a good correlation between those rates of cooling when viability begins to decline and the onset-cooling rate for non equilibrium freezing. This suggests that the

common factor that determines viability on thawing is the solidification behaviour of the glycerol solution at different rates of cooling. The differences observed with the different species may reflect the sensitivity of the cells to tolerate and osmotic shock at low temperature.

The results described in this paper suggest that it is now appropriate for new models to be developed that exclude the formation of intracellular ice. In particular the effects of cooling rate on the composition of the freeze concentrated matrix at any temperature during cooling should be included in any such models. This more realistic modelling should predict optimum methods of cryopreservation of spermatozoa and lead to improved practical cryopreservation protocols.

References

- [1] Ablett S, Izzard MJ, Lillford PJ. Differential scanning calorimetric study of frozen sucrose and glycerol solutions. *J Chem Soc Faraday Trans* 1992;88:789–94.
- [2] Ball BL, Vo A. Osmotic tolerance of equine spermatozoa and the effects of soluble cryoprotectants on equine sperm motility, viability and mitochondrial membrane potential. *J Androl* 2001;22:1061–9.
- [3] Baudot A, Odagescu V. Thermal properties of ethylene glycol aqueous solutions. *Cryobiology* 2004;48:283–94.
- [4] Boutron P. Levo- and dextro-2,3-butanediol and their racemic mixture: very efficient solutions for vitrification. *Cryobiology* 1990;27:55–69.
- [5] Boutron P, Kaufmann A. Stability of the amorphous state in the system water 1,2-propanediol. *Cryobiology* 1979;16:83–9.
- [6] Bronshteyn VL, Steponkus PL. Nucleation and growth of ice crystals in concentrated solutions of ethylene glycol. *Cryobiology* 1995;32:1–22.
- [7] Courtens JL, Paquignon M. Ultrastructure of fresh, frozen and frozen-thawed spermatozoa of the boar. In: Johnson LA, Larsson K, editors. *Proceedings of the First International Conference on Deep Freezing of Boar Semen*. 1985. p. 61–87.
- [8] Curry MR. Cryopreservation of semen from domestic livestock. *Rev Reprod* 2000;5:46–52.
- [9] Curry MR, Millar JD, Watson PF. Calculated optimal cooling rates for ram and human sperm cryopreservation fail to conform with empirical observations. *Biol Reprod* 1994;51:1014–21.
- [10] Davies GJ. *Solidification and casting*. London: Applied Science Publishers Ltd.; 1973. pp. 55–58.
- [11] Devireddy RV, Swanlund DJ, Roberts KP, Pryor JL, Bischof JC. The effect of extracellular ice and cryoprotective agents on the water permeability parameters of human sperm plasma membrane during freezing. *Hum Reprod* 2000;15:1125–32.
- [12] Devireddy RV, Swanlund DJ, Olin T, Vincente W, Troedsson MHT, Bischof JC, et al. Cryopreservation of equine sperm: optimal cooling rates in the presence and absence of cryoprotective agents determined using differential scanning calorimetry. *Biol Reprod* 2002;66:222–31.
- [13] Devireddy RV, Swanlund DJ, Alghamdi AS, Duoos LA, Troedsson MHT, Bischof JC, et al. Measured effect of collection and cooling conditions on the motility and the water transport parameters at sub-zero temperatures of equine spermatozoa. *Reproduction* 2000;5:643–8.

- [14] Ecot P, Vidament M, De Mornac A, Perigault K, Clement F, Palmer EJ. Freezing of stallion semen: interactions among cooling treatments, semen extenders and stallions. *Reprod Fertil* 2000;56:141–50.
- [15] Faszer K, Draper D, Green JE, Morris GJ, Grout BWW. Cryopreservation of horse semen under laboratory field conditions using a stirling cycle freezer. *Cryoletters* 2006;27:179–84.
- [16] Fonseca F, Marin M, Morris GJ. Stabilization of frozen *Lactobacillus bulgaricus* in glycerol suspensions: freezing kinetics and storage temperature effects. *Appl Environ Microbiol* 2006;72:6472–82.
- [17] Franks F. Properties of aqueous solutions at subzero temperatures. In: Franks F, editor. *Water a comprehensive treatise. Water and aqueous solutions at subzero temperatures*, vol. 7. NY: Plenum Press; 1982. p. 292–309.
- [18] Gilmore JA, Liu J, Woods EJ, Peter AT, Crister JK. Cryoprotective agent and cryoprotective effects on human sperm membrane permeabilities; convergence of theoretical and approaches for optimal cryopreservation methods. *Hum Reprod* 2000;15:335–43.
- [19] Henry MA, Noiles EE, Gao DY, Mazur P, Crister JK. Cryopreservation of human spermatozoa. IV. The effects of cooling rate and warming rate on the maintenance of motility, plasma membrane integrity and mitochondrial function. *Fertil Steril* 1993;60:911–8.
- [20] Hey MJ, MacFarlane DR. Crystallisation of ice in aqueous solutions of glycerol and dimethyl sulfoxide. *Cryobiology* 1996;33:215–6.
- [21] Hey MJ, MacFarlane DR. Crystallisation of ice in aqueous solutions of glycerol and dimethyl sulfoxide 2: ice crystal growth kinetics. *Cryobiology* 1998;37:119–30.
- [22] Leibo SP, Bradley L. Comparative cryobiology of mammalian spermatozoa. In: Cagnon C, editor. *The male gamete: from basic knowledge to clinical applications*. Vienna IL, USA: Cache River Press; 1999. p. 501–16.
- [23] Luyet B. On various phase transitions occurring in aqueous solutions at low temperatures. *Proc NY Acad Sci* 1965;125:549–69.
- [24] Mantovani R, Rota R, Falamo ME, Bailoni L, Vincenti L. Comparison between glycerol and ethylene glycol for the cryopreservation of equine spermatozoa: semen quality assessment with standard analyses and with the hypoosmotic swelling test. *Reprod Nutr Dev* 2002;42:217–26.
- [25] Mazur P. Principles of cryobiology. In: Fuller BJ, Lane N, Benson EE, editors. *Life in the frozen state*. Boca Raton, FL, USA: CRC Press; 2004. p. 3–65.
- [26] Mazur P, Koshimoto C. Is intracellular ice formation the cause of death of mouse sperm frozen at high cooling rates? *Biol Reprod* 2002;66:1485–90.
- [27] Moran DM, Jasko JD, Squires EL, Amann RP. Determination of temperature and cool rate induced cold shock in stallion spermatozoa. *Theriogenology* 1992;38:999–1012.
- [28] Morris GJ. Rapidly cooled human sperm: no evidence of intracellular ice formation. *Hum Reprod* 2006;21:2075–83.
- [29] Morris GJ, Acton E, Avery S. A novel approach to sperm cryopreservation. *Hum Reprod* 1999;14:1013–21.
- [30] Morris GJ, Richens HE. Improved methods for controlled rapid cooling of cell suspensions. *CryoLetters* 2004;25:265–72.
- [31] Morris GJ, Goodrich M, Acton E, Fonseca F. The high viscosity encountered during freezing in glycerol solutions: effects on cryopreservation. *Cryobiology* 2006;52:323–34.
- [32] Noiles EE, Mazur P, Watson PF, Kleinhans FW, Crister JK. Determination of water permeability coefficient for human spermatozoa and its activation energy. *Biol Reprod* 1993;48:99–109.
- [33] Pommer AC, Rutllant J, Meyers SA. The role of osmotic resistance on equine spermatozoa function. *Theriogenology* 2002;58:1373–84.
- [34] Rodriguez-Martinez H, Ekwall H. Electron microscopy in the assessment of cryopreserved spermatozoa viability. *Microsc Anal* 1988;(May Issue):29–31.
- [35] Samper JC, Morris CA. Current methods for stallion cryopreservation: a survey. *Theriogenology* 1998;49:895–903.
- [36] Sherman JK, Liu KC. Ultrastructure before freezing, while frozen, and after thawing in assessing cryoinjury of mouse epididymal spermatozoa. *Cryobiol* 1988;19:503–10.
- [37] Squires EL. Integration of future biotechnologies into the equine industry. *Anim Reprod Sci* 2005;89:187–98.
- [38] Vali G. Principles of ice nucleation. In: Lee RE, Warren GJ, Gusta LV, editors. *In biological ice nucleation and its applications*. APS Press; 1989. p. 1–28.
- [39] Vigier G, Thollet G, Vassoille R. Cubic and hexagonal ice formation in water-glycerol mixture (50% w/w). *J Cryst Growth* 1987;84:309–15.